European Journal of Pharmaceutics and Biopharmaceutics 79 (2011) 601–611

Contents lists available at SciVerse ScienceDirect

European Journal of Pharmaceutics and Biopharmaceutics

journal homepage: www.elsevier.com/locate/ejpb

Research paper

Different modalities of NaCl osmogen in biodegradable microspheres for bone deposition of risedronate sodium by alveolar targeting

Maha Nasr [a,*], Gehanne A.S. Awad [a], Samar Mansour [a], Ismail Taha [b], Abdelhamid Al Shamy [a], Nahed D. Mortada [a]

[a] Pharmaceutics Department, Faculty of Pharmacy, Ain Shams University, Cairo, Egypt
[b] Hot Lab. Center, Atomic Energy Authority, Cairo, Egypt

ARTICLE INFO

Article history:
Received 25 January 2011
Accepted in revised form 22 July 2011
Available online 29 July 2011

Keywords:
Risedronate
Surface engineer
Microspheres
Pulmonary
Osmogen

ABSTRACT

Risedronate sodium was formulated into polylactide-co-glycolic acid microspheres for pulmonary delivery using the w/o/w double emulsion technique. Sodium chloride was used as osmogen in either the internal or external aqueous phase to surface-engineer the particles to achieve favorable properties. The prepared microspheres were characterized for the surface morphology, entrapment efficiency, *in vitro* release behavior, particle size, surface area, aerodynamic as well as powder flow properties. Furthermore, the safety of the drug and the selected formula were assessed by MTT viability test performed on Calu-3 cell line as well as histopathological lung tissue examination. A novel *in vivo* approach based on the radiolabeling of risedronate sodium with I^{125} was developed in order to assess its deposition in the bones of male albino rats. The majority of the prepared microspheres exhibited high entrapment efficiency, sustained release profile up to 15 days, suitable geometric and aerodynamic particle sizes as well as good flow properties. The safety of the drug and the selected formula were proven by the high cell viability percentage of Calu-3 cells as well as the normal lung histology after intra-tracheal administration. The *in vivo* study showed high bone deposition for risedronate sodium following the pulmonary route, suggesting that it could be utilized as an alternative route of administration for delivery of bisphosphonates.

1. Introduction

Porous or surface modified polylactide-co-glycolide (PLGA) microspheres are commonly employed as a suitable carrier for pulmonary administered drugs owing to their biocompatibility, controlled release behavior, and their well-known safety profile [1].

Various approaches have been attempted in the literature to incorporate water soluble drugs into biodegradable microspheres at high loading. However, the double (w/o/w) emulsion method remains the most commonly used method for achieving such purpose [2]. Upon using osmogens as NaCl in the preparation of these microparticles, the organic phase of a w/o/w emulsion acts as semipermeable membrane allowing the passage of water across the organic phase [3,4], which in turn leads to the production of diverse modalities of microspheres, differing in their morphology, entrapment efficiency properties, release capabilities, and aerodynamic deposition in the lung.

Bisphosphonates (BPs), the gold-standard pharmacological treatment of osteoporosis [5], suffer extremely low bioavailability (less than 1%) upon their oral intake owing to their high polarity and hydrophilicity. Furthermore, they exhibit several gastric and esophageal side effects such as erosive esophagitis, gastritis, and ulcers. These adverse effects are hypothesized to be caused by the reflex of the acidic gastric contents along with the undissolved drug crystals back to the esophagus, exposing it to the free acid form of the drug, or due to the exacerbation of an existing esophageal disorder [6,7]. They might also be caused by the local reaction of the mucosa upon contact with the concentrated form of the drug [8–10]. The local tissue damage and irritation at the sites of injection precluded the use of intra-muscular and subcutaneous routes of administration for delivery of BPs. Slow release of BPs is also critical, since it was reported that rapid injection of BPs can lead to renal failure due to the formation of complexes with calcium in the blood, which are held back in the kidney [10]. A model BP, risedronate sodium (RS), was used in our study, as it possessed a high anti-resorptive activity while causing less incidence of gastric damage [11].

Therefore, the aim of our work was to test the possibility for delivery of RS through an alternative route (the pulmonary route), taking advantage of the neutral pH of the lung environment with

* Corresponding author. Ain Shams University, Faculty of Pharmacy, Department of Pharmaceutics, Monazamet El Wehda El Afrikia St., El Abbassia, Cairo, Egypt. Tel.: +20 20103450279; fax: +20 24051107.
E-mail address: maha2929@gmail.com (M. Nasr).

0939-6411/$ - see front matter © 2011 Elsevier B.V. All rights reserved.
doi:10.1016/j.ejpb.2011.07.010

the possibility of using small dose to minimize possible local mucosal irritation. Different modalities for NaCl as osmogen through changing its concentration in the internal and external aqueous phases were attempted, in which the influence of the relative difference in osmotic pressure on the produced microspheres was studied through several experimental parameters. Sodium chloride was used as the osmogen of choice based on preliminary study conducted in our laboratory [12]. Cellular toxicity using MTT assay on Calu-3 cells as well as histological examination of lung tissue was performed in order to assess the safety of the optimized formula. In addition, instead of using the traditional chromatographic methods to test the bioavailability of our optimized formula, a novel radiolabeling technique was utilized to calculate the percentage of RS directly deposited in the bones after pulmonary administration.

2. Materials and methods

2.1. Materials

Risedronate sodium was gifted by SPIC Pharma. Co., India. PLGA 50:50 and 75:25 of molecular weights 150,000 and 95,000 g/mole, respectively, were gifted by PURAC Biomaterials Co., the Netherlands. Polyvinyl alcohol (Mowiol®4-88) Molecular weight 31,000, MTT: 3-(4,5-dimethylthiazol-2-yl)-2,5-diphenyl-tetrazolium bromide, HEPES buffer, fetal calf serum, gentamycin, phosphate buffered saline tablets (PBS), dimethyl sulfoxide (DMSO), sodium dodecyl sulfate (SLS), sodium pentobarbital, and chloramine-T were purchased from Sigma Chemical Co., USA. Dichloromethane (DCM), sodium hydroxide, disodium hydrogen phosphate, potassium dihydrogen phosphate, and sodium chloride (purity ⩾99%) were purchased from Adwic, El Nasr pharmaceutical company, Egypt. Spectra/Por dialysis membrane, 12,000–14,000 molecular weight cutoff, was purchased from Spectrum Laboratories Inc., Canada. L-glutamine GIBCO® was purchased from Invitrogen Co., USA. Minimum Essential Medium Eagle (MEM medium) and Trypsin–EDTA were purchased from LONZA Co., Belgium. $K^{125}I$ was purchased from H1121 Budapest, Konkoly-Thege Miklòs ùt 29–33, as no carrier added solution of radionuclidic purity >99%. All other chemicals were obtained as reagent-grade products.

2.2. Preparation of RS loaded PLGA microspheres using NaCl as osmogen

RS loaded PLGA microspheres were prepared by w/o/w double emulsion technique based on the results of the entrapment optimization study done in a previous work in our laboratory [12]. Briefly, PLGA polymer (500 mg) of either type 50:50 or 75:25 was dissolved in 8 ml DCM. RS (50 mg) was dissolved in 1600 μl of 1% PVA solution as the internal aqueous phase, which was added to the organic polymer solution and homogenized for 30 s at 8000 rpm using a homogenizer (Heidolph DIAX 900, Germany). The primary emulsion was further emulsified into 150 ml of 1% PVA solution at 8 °C and stirred at 1500 rpm using a magnetic stirrer (IKAMAG®, model C-MAG HS 7, Germany) for 4 h. Sodium chloride was added in various concentrations in the internal or external aqueous phase or both. Table 1 shows the composition of different microsphere groups. The polymeric particles were centrifuged at 7000 rpm for 5 min (Hermle Labortechnik GmBH, model Z216MK, Germany) and washed with three portions of distilled water. The microspheres were vacuum-dried for 24 h at ambient conditions and then stored in a desiccator for further investigations.

The amount of residual DCM was then determined using a gas chromatographic system equipped with flame ionization detector (Shimadzu, model GC-17A). The microspheres were dissolved in a standard solution (10 mg microspheres in 10 ml DMF), the oven temperature was 80 °C, injector temperature was 150 °C, and the detector temperature was 200 °C [13]. The residual solvent content was calculated using a standard curve constructed with known dilutions of DCM.

2.3. Characterization of the prepared microspheres

2.3.1. Determination of RS entrapment efficiency into the prepared microspheres

The EE% of RS in PLGA microspheres was determined using an extraction procedure in alkaline medium [12]. A constant amount of microspheres (10 mg) was dissolved in 5 ml DCM. RS was then extracted by 20 ml of 1 M sodium hydroxide solution on three divided portions and assayed spectrophotometrically in the NaOH solution at 262 nm (UV-1601 PC, Shimadzu, Japan) according to the following equation:

$$\mathrm{EE}\% = \frac{\text{Amount of drug in microspheres}}{\text{Amount of drug used in the formulation}} \times 100 \quad (1)$$

2.3.2. Scanning electron microscopy (SEM)

The morphology and surface characteristics of microspheres were examined by SEM (JSM 5500, Jeol, Japan). The samples were mounted onto aluminum stubs using double-sided adhesive tape onto which the microspheres were applied and sputter coated with thin layer of gold particles for 1 min (SPI-Module, USA) prior to examination by SEM at 10 kV.

2.3.3. Particle size analysis

The particle size was measured using laser diffraction particle size analyzer (Mastersizer X, Malvern Instruments Ltd., UK). The prepared microspheres were placed in a sample holding cell with stirrer so that the sample, diluted with distilled water (refractive index 1.33), was stirred to keep the sample in suspension while particle size was being measured. The polydispersity of the particles was expressed in terms of the SPAN index according to the following equation:

$$\text{SPAN index} = \frac{D[v,90] - D[v,10]}{D[v,50]} \quad (2)$$

where $D[v,90]$, $D[v,10]$, and $D[v,50]$ are the respective diameters at 90%, 10%, and 50%.

2.3.4. Particle flow and aerodynamic properties

Powder density was estimated by tapped density measurements. A known weight (150 mg) of PLGA microspheres was transferred to a graduated 1 ml syringe, and the initial volume was recorded [14,15]. The syringe was tapped up to a volume plateau [16]. Tapped density of the particles was calculated as the ratio between the sample weight (g) and the final volume (ml) occupied after 1250 tappings [17]. The theoretical mass mean aerodynamic diameter ($\mathrm{MMAD_{th}}$) of the particles was calculated using the equation:

$$\mathrm{MMAD_{th}} = d(\rho/\rho_o X)^{1/2} \quad (3)$$

where d is the geometric mean diameter obtained from particle size analysis, ρ is the tapped density, ρ_o is the reference density of 1 g/cm^3, and X is the shape factor, which equals to 1 for a sphere [17,18].

Furthermore, to obtain information about the microparticles' compressibility and flowability properties, the compressibility index (Carr's index) was estimated by calculating the relative percent difference between bulk and tapped density as stated by the US Pharmacopoeia:

Table 1
Composition of RS loaded microspheres prepared with NaCl osmogen.

Microsphere group	Formula code	PLGA type	NaCl concentration in internal aqueous phase (w/v) (%)	NaCl concentration in external aqueous phase (w/v) (%)
Group I	F1	50:50	1	0
	F2	50:50	1	0.5
	F3	75:25	1	0.5
	F4	50:50	5	1
	F5	75:25	5	1
	F6	50:50	5	0.5
	F7	75:25	5	0.5
Group II	E1	50:50	1	1
	E2	75:25	1	1
	E3	50:50	0.5	0.5
	E4	50:50	5	5
Group III	S1	50:50	1	5
	S2	75:25	1	5
	S3	50:50	0.5	1
	S4	75:25	0.5	1
	S5	50:50	0.5	5
	S6	75:25	0.5	5

$$\text{Carr's index} = \left(1 - \frac{\rho i}{\rho}\right) \times 100 \quad (4)$$

where ρ and ρ_i are tapped and bulk densities of the powder, respectively. Based on reported values for Carr's index, powder flowability is defined as follows: 5–12% excellent; 12–18% good; 18–21% fair; 21–25% poor, fluid; 25–32% poor, cohesive; 32–38%, very poor; >40% extremely poor [16,19].

2.3.5. In vitro drug release from microspheres

An *in vitro* drug release method similar to the one attempted by other co-workers [20,21] was used. A Franz diffusion cell (Variomag, Telesystem, H + P Labortechnik, Germany) with a diffusion area of 1.77 cm^2 fitted with a cellulose acetate membrane was used to monitor the *in vitro* drug release. The receptor compartment contained 7.5 ml phosphate buffered saline pH 7.4 (0.154 mM) maintained at 37 °C by a circulating water jacket and constantly stirred at 150 rpm with a small magnetic bar. Microparticles equivalent to 1 mg RS were mounted on the membrane and dispersed in 200 μl PBS in the donor compartment. At selected time intervals (1, 2, 4, 6, 8, 24, and 48 h, as well as 7, 10, and 15 days), 500 μl was sampled from the receptor compartment and replaced with an equal volume of fresh receptor solution. As a control, the release of 1 mg RS solution was performed. The quantity of RS released was determined using UV spectrophotometry at 262 nm. The *in vitro* drug release data were fitted using zero, first, Higuchi diffusion. Further fitting using Korsmeyer–Peppas equation [22] was performed when necessary according to the following equation:

$$\frac{Mt}{M\infty} = Kt^n \quad (5)$$

where Mt and $M\infty$ correspond to the amount of drug released at time t and ∞, respectively, k is the kinetic constant, t is the release time, and n is the diffusional component for drug release.

2.3.6. Measurement of the true density and specific surface area (SSA) of the microspheres

The true density of the microspheres was calculated through gas displacement using helium pycnometer (Quantachrome, ultrapyconmeter 1000, USA). Approximately 500 mg of microspheres was weighed into the sample holder after calibration of the pycnometer using standard stainless steel spheres supplied by the manufacturer, and the volume of the helium gas displaced by the powder was measured giving the true (skeletal) density [23].

The specific surface area (SSA) of the microspheres was calculated according to the following equation [24]:

$$\text{SSA} = \frac{6}{\rho D[3,2]} \quad (6)$$

where ρ is the true density of the microspheres measured using the helium pycnometer, and D [3,2] is the surface area weighted mean diameter.

2.3.7. Differential scanning calorimetry (DSC)

The thermal properties of RS, PLGA 50:50, and the selected RS loaded microspheres formulae were investigated using a differential scanning calorimeter calibrated with indium (DC-60, Shimadzu, Japan). Samples (3–5 mg) were sealed in aluminum pans with lids and heated at a rate of 10 °C/min to a temperature of 300 °C, using dry nitrogen as carrier gas with a flow rate of 25 ml/min.

2.4. Cytotoxicity evaluation by MTT assay

Cytotoxicity of the selected formulation was determined by MTT assay in Calu-3 cells. In this test, Calu-3 cells were grown on MEM medium supplemented with 10% heat-inactivated fetal calf serum, 1% L-glutamine, HEPES buffer, and 50 μg/ml gentamycin. All cells were maintained at 37 °C in a humidified atmosphere (95% RH) with 5% v/v CO2 (Humid CO2 incubator, Shel lab 2406, USA) [25]. The cells were seeded in 96-well plate at a cell concentration of 1×10^4 cells per well in 100 μl of growth medium. Different concentrations of PLGA particles from 0.03125 to 2 mg/ml were prepared in 100 μl of the growth medium and added to the cell monolayers with incubation for 24 h. Twenty μl MTT solution (5 mg/ml in PBS, pH 7.4) was added to the cells followed by incubation at 37 °C for 4 h [18]. The medium was then removed, and the formazan crystals formed were solubilized with 100 μl dimethyl sulfoxide (DMSO). The absorbance was read at 570 nm on a microplate reader (Tecan Sunrise®, Switzerland). Both sodium dodecyl sulfate and RS in solution form were used as controls. The cell viability percentage was calculated according to the following equation:

$$\text{Cell viability}\% = \frac{A(\text{test})}{A(\text{control})} \times 100 \quad (7)$$

where A (test) is the absorbance obtained for each of the concentrations of the test substance, and A (control) is the absorbance obtained for untreated cells (incubated with medium only). The latter reading was assumed to correspond to 100% cell viability.

2.5. Histopathological examination of lung tissue

Autopsy lung samples were taken after 24 h postdosing from three groups of male albino rats (300–350 g). Group I was administered phosphate buffered saline intra-tracheally as a negative control, group II was administered 1 mg of the drug RS intra-tracheally dissolved in phosphate buffered saline, and group III was administered an amount of RS microspheres of the selected formula (S5) equivalent to 1 mg RS intra-tracheally dispersed in phosphate buffered saline as well. Autopsy samples were fixed in 10% formol saline for 24 h. Washing was done in tap water, and then, serial dilutions of alcohol were used for dehydration. Specimens were cleared in xylene and embedded in paraffin at 56 °C in hot air oven for 24 h. Paraffin bees wax tissue blocks were prepared for sectioning at 4 μm by slidge microtome (Rotary Leica RM2245, USA). The obtained tissue sections were collected on glass slides, deparaffinized, and stained by hematoxylin and eosin stains

for histopathological examination through the electric light microscope (Axiostar plus, Zeiss, USA).

2.6. In vitro aerosolization study

The selected microspheres formula (S5) was examined for its aerosolization properties using Next Generation Impactor (NGI) (Copley M170, UK), which was considered the impactor of choice for DPI testing [26]. Microspheres in an amount equivalent to 1 mg RS were filled into size three capsule, which was then placed in Aerolizer® inhaler device (Novartis, UK). Deposition behavior of the microspheres was performed at a flow rate 30 L/min for 8 s using a vacuum pump (Copley HCP5, UK). The microspheres deposited in each stage of the NGI were collected using 1 N NaOH as a collecting solvent and analyzed for drug content using the method previously described in Section 2.3.1. The microspheres depositing on the inhaler, adapter, preseparator (PS), and remaining in the capsule were also analyzed for drug content. The emitted fraction (EF%) was determined gravimetrically [27] using the following equation:

$$EF\% = \left(\frac{m_{full} - m_{empty}}{m_{powder}}\right) \times 100 \quad (8)$$

where m_{full} and m_{empty} refer to the weight of the capsule before and after the aerosolization, respectively, and m_{powder} is the initial weight of the microspheres placed in the capsule.

The fine particle fraction (FPF%) was calculated according to the following equation [27]:

$$FPF_{<4.46\ \mu m}(\%) = \left(\frac{\text{Amount of drug in microspheres with aerodynamic diameters} < 4.46\ \mu m}{\text{Sum of the amount f drug collected from all NGI stages} + \text{throat} + \text{adapter}}\right) \times 100 \quad (9)$$

The experimental mass median aerodynamic diameter (MMAD) of the aerosolized formula was calculated by analyzing the amount of drug deposited in different NGI stages.

2.7. Radiolabeling of RS using $K^{125}I$

2.7.1. Radioiodination labeling technique

RS was dissolved in distilled water at a concentration of 50 mg/2 ml, and the pH was adjusted to nine using phosphate buffer. Freshly prepared chloramine-T solution (50 μg/5 μl) was added to RS solution followed by the addition of 3.5 m Ci $K^{125}I$ at 25 °C. After 1 h, the reaction was quenched through the reduction of remaining chloramine-T using (150 μg/5 μl) $Na_2S_2O_5$. The labeled compound was investigated using electrophoresis analysis and thin layer chromatography.

2.7.2. Calculating the reaction yield using electrophoresis and thin layer chromatography

Electrophoresis was done using a programmable electrophoresis power supply (E.C. 3000p-series 90, E-C Apparatus corporation, St. Petersburg, USA) using cellulose acetate strips (45 cm). Cathode and anode poles as well as application points were indicated on these strips and were subsequently moistened with buffer solution (0.05 M phosphate buffer pH 7). Ten microliters of the reaction mixture samples was set on the strips and introduced in the electrophoresis chamber at a distance of 10 cm from the cathode. Current at 300 V was applied for 1½ h. Developed strips were dried and cut into 1 cm segments, then counted by a well-type NaI scintillation counter. The radiochemical yield was calculated as the ratio of the radioactivity of the labeled product to the total radioactivity:

$$\%\ \text{Radiochemical yield of}\ ^{125}I - RS = \frac{Peak activity\ of\ 125I - RS}{Total\ activity} \times 100 \quad (10)$$

The radiochemical yield of ^{125}I-RS was further confirmed using thin layer chromatography (TLC) [28]. Silica gel 60 supported on aluminum sheets (20 × 2 cm^2) was activated by heating at 110 °C for 2 h. Volumes of 10 μL were placed 2 cm from the base of TLC, then developed using mobile phase chloroform/ethanol/ammonia (90:10:0.5). The strips were dried under inert N_2, cut into 1 cm segments, and then assayed for radioactivity. The retention factor was calculated according to the following equation, and the radiochemical yield of I_{125} labeled RS was determined as stated in Eq. (10):

$$R_F = \frac{Distance\ travelled\ by\ 125I\text{-}RS}{Distance\ travelled\ by\ solvent} \quad (11)$$

2.8. In vivo determination of the amount of bone deposited ^{125}I-RS

The bone deposition study was carried out on four groups of male albino rats of six rats each weighing 300–350 g. The animals were fed a normal diet and water *ad libitum* in a constant temperature environment of 25 °C, and a period of 7 days was allowed for acclimatization of rats before any experimental manipulation was undertaken. Rats were anesthetized using intra-peritonial injection of sodium pentobarbital (32 mg/kg), followed by orotracheal instillation of the selected ^{125}I-RS labeled formula dispersed in 200 μl phosphate buffered saline (pH 7.4).

The selected formula (S5) was administered intra-tracheally, in an amount equivalent to 1 mg ^{125}I-RS to groups I and II, which were sacrificed after 24 h and 7 days postdosing, respectively. Groups III and IV were injected an amount of 1 mg of the drug ^{125}I-RS in solution form in the tail vein and were sacrificed also after 24 h and 7 days, respectively. Samples of fresh blood were taken immediately before killing the rats. The bones and thyroid glands were dissected and placed in pre-weighed counting vials, and the activity was counted and expressed as a percentage of the inhaled or injected activity. Blood and bone were assumed to be 7% and 12% of the total rat body weight, respectively [29]. Corrections were made for background radiation during experiment. The percentage of injected/inhaled dose (% I.D.) was calculated according to the following equation:

$$\%\text{I.D.} = \frac{C_2 \times W_2 \times 100}{W_1 \times S} \quad (12)$$

where C_2 is the sample count per unit time, W_2 is organ mass (g), W_1 is sample mass (g), and S is the activity of the injected/inhaled dose expressed as count per unit time. All animal procedures were approved by the Ethics Committee of the Faculty of Pharmacy Ain Shams University, in accordance with the guidelines of the Experiments and Advanced Pharmaceutical Research Unit (EAPRU).

2.9. Statistical analysis

All experiments were repeated at least three times. Results were expressed as mean ± standard deviation (S.D) or standard error (S.E). One-way ANOVA followed by Tukey Kramer test was done using GraphPad® Instat software. A difference between

means was considered significant if the p-value was less than or equal to 0.05.

3. Results and discussion

3.1. Preparation of RS loaded PLGA microspheres using NaCl as osmogen

Sodium chloride is commonly used as porogen owing to its osmotic effects. It is well known that water molecules may pass from one aqueous phase to the other, based on the difference in osmotic pressure [4]. Materials such as electrolytes and drugs in either aqueous phases are also known to exert a similar osmotic effect [3]. Therefore, in our study, the osmotic gradient was varied through changing the amount of NaCl in the internal and external aqueous phases, in order to study its effect on EE%, and accordingly, two groups of microspheres were prepared with different concentrations of NaCl in the internal/external phases (groups I and III), and one group was prepared with equal concentration of NaCl on both sides (group II), serving as our control group. Upon exceeding the 5% NaCl concentration in the internal aqueous phase, rapid transfer of water occurred from the outside toward the internal aqueous phase leading to bursting of the microspheres; therefore, a maximum limit of 5% NaCl was used in our present study.

No residual DCM was detected using gas chromatography in the prepared microspheres, which complies with the requirements of the USPXXVIII for volatile impurities [13].

3.2. Determination of RS entrapment efficiency into the prepared microspheres

From the results in Table 2, it can be observed that microspheres prepared using PLGA 50:50 had general significantly higher EE% ($P < 0.05$) than their counterparts prepared using PLGA 75:25. This could be attributed to the fact that PLGA 50:50 with its higher glycolide content is more hydrophilic than PLGA 75:25, allowing better entrapment of hydrophilic RS into the microspheres [30]. Table 2 and Fig. 1 show that with both PLGA types, the increase in NaCl percentage in the external aqueous phase, while keeping its concentration constant in the internal aqueous phase, resulted in a significant increase in RS EE% ($P < 0.01$). NaCl in the external phase provided an effective mechanical barrier to drug transfer and kept the internal aqueous phase droplets small, which is considered to be an important prerequisite for drug encapsulation [4]. Additionally, it was reported that the high concentration of NaCl in the external phase would speed up the process of polymer precipitation, which in turn causes the solid polymer to act as diffusion barrier to the drug. Moreover, the higher water solubility of NaCl in comparison with RS would contribute with the other factors to decrease the escape of RS into the external medium [30,31]. This effect was more apparent at the highest NaCl concentration in the external phase.

On the contrary, the increase in the percentage of NaCl in the internal phase resulted in a general significant decrease in the EE% for RS in PLGA microspheres ($P < 0.05$). The high salt concentration, in the internal aqueous phase, is expected to have forced water to pass along the osmotic pressure gradient, from the external to the internal phase, resulting in swelling of the internal droplets and of the embryonic microspheres. Consequently, destabilization of the w/o/w emulsion occurred with delay of polymer coacervation and the immobilization and encapsulation of the inner aqueous phase within the spherical polymer matrix. This hindrance of encapsulation, in addition to the occasional rupture of the polymeric layer caused by the influx of water, would lead

Table 2
Characterization of RS loaded PLGA microspheres prepared using NaCl as osmogen.

Group	Formula code	EE% mean ± S.D.	Distribution modal size (μm) mean ± S.D.	SPAN index mean ± S.D.	Tapped density (g/ml) mean ± S.D.	Carr's index mean ± S.D.	$MMAD_{th}$ mean ± S.D.	Cumulative amount released% after 15 days mean ± S.D.
I	F1	17.23 ± 0.16	8.39 ± 0.51	1.67 ± 0.06	0.323 ± 0.03	35.30 ± 5.42	4.76 ± 0.21	N.D.*
	F2	24.15 ± 1.04	8.39 ± 0.36	1.65 ± 0.04	0.325 ± 0.02	35.09 ± 3.51	4.78 ± 0.14	48.38 ± 0.98
	F3	21.98 ± 0.78	6.84 ± 0.53	1.65 ± 0.08	0.319 ± 0.02	32.86 ± 6.60	3.86 ± 0.14	43.81 ± 3.60
	F4	36.81 ± 3.32	(4.27, 10.47) ± 0.89	2.87 ± 0.39	0.313 ± 0.01	32.65 ± 0.92	N.D.‡	50.66 ± 6.80
	F5	34.40 ± 1.02	8.41 ± 0.42	1.38 ± 0.04	0.315 ± 0.02	33.10 ± 6.14	4.72 ± 0.15	45.13 ± 2.43
	F6	21.21 ± 1.07	(6.8, 10.48) ± 0.92	3.02 ± 0.41	0.313 ± 0.00	30.40 ± 2.06	5.86 ± 0.05	58.97 ± 0.26
	F7	17.39 ± 1.96	(7.22, 10.23) ± 0.30	1.70 ± 0.30	0.308 ± 0.01	29.26 ± 3.39	5.68 ± 0.09	N.D.*
II	E1	38.27 ± 0.64	(4.81, 6.83) ± 0.25	1.52 ± 0.02	0.344 ± 0.02	34.43 ± 4.83	4.00 ± 0.13	34.93 ± 2.08
	E2	24.42 ± 1.88	5.58 ± 0.47	1.58 ± 0.05	0.403 ± 0.01	44.28 ± 3.76	3.54 ± 0.07	23.14 ± 1.83
	E3	25.30 ± 1.38	6.77 ± 0.36	1.48 ± 0.04	0.338 ± 0.02	34.56 ± 3.85	3.93 ± 0.12	35.19 ± 1.13
	E4	57.12 ± 1.45	5.71 ± 0.54	1.63 ± 0.05	0.363 ± 0.03	40.85 ± 5.22	3.44 ± 0.13	31.69 ± 2.20
III	S1	81.19 ± 2.86	(3.99, 5.58) ± 0.44	1.39 ± 0.07	0.387 ± 0.03	17.40 ± 1.10	3.47 ± 0.15	67.79 ± 0.94
	S2	68.85 ± 2.90	4.53 ± 0.68	1.35 ± 0.14	0.383 ± 0.02	20.19 ± 5.44	2.80 ± 0.06	60.22 ± 3.53
	S3	55.71 ± 2.81	(3.97, 5.59) ± 0.21	1.25 ± 0.20	0.392 ± 0.01	19.80 ± 4.03	3.50 ± 0.03	63.59 ± 3.21
	S4	18.19 ± 1.01	4.48 ± 0.58	1.84 ± 0.25	0.391 ± 0.02	17.67 ± 1.77	2.80 ± 0.08	N.D.*
	S5	95.37 ± 2.22	3.68 ± 0.69	1.28 ± 0.03	0.372 ± 0.03	16.09 ± 1.01	2.24 ± 0.08	64.09 ± 3.91
	S6	43.90 ± 2.31	4.45 ± 0.85	1.22 ± 0.04	0.373 ± 0.01	17.78 ± 3.74	2.72 ± 0.05	46.20 ± 2.56

Underlined numbers in distribution modal size represent predominant population.
‡ N.D.: Not determined since F4 showed 2 equally predominant populations.
* N.D.: Not determined since formulae F1, F7, and S4 had very low EE% values (less than 20%).

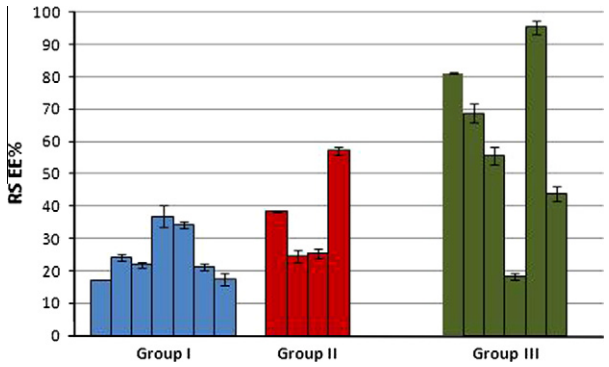

Fig. 1. Effect of the osmotic pressure difference created by NaCl concentration on the EE% of RS microspheres. (For interpretation of the references to colour in this figure legend, the reader is referred to the web version of this article.)

to the release of the inner phase into the external water phase and the loss of drug during encapsulation [4].

3.3. Scanning electron microscopy (SEM)

Formulae F4, E1, and S5 were chosen as representatives of groups I, II, and III, respectively. F4 showed that most of the microspheres displayed a porous surface as obvious in Fig. 2. The increased osmotic pressure in the internal aqueous phase due to the increased NaCl concentration caused particle swelling, with the appearance of spongy-like structures [4] as illustrated by the arrows in Fig. 2a. Upon equilibrating the NaCl concentration in the internal and external aqueous phases in formula E1, the microspheres exhibited shallow surface dimpling with only occasional appearance of pores, as evident in Fig. 3a and illustrated by the arrows. This confirms the osmotic properties of RS, similar to what was reported for pamidronate disodium, which is a BP drug similar in properties to RS [32]. Upon increasing the NaCl concentration in the external aqueous phase in case of formula S5, shrinkage of the particles occurred resulting in deep surface dimpling, along with the exhibition of a compact and dense microspheres surface. The flux of water from the internal to the external aqueous phase accompanying the increased enternal NaCl concentration caused the microspheres to have a notched surface as displayed in Fig. 4. The addition of NaCl in the external phase was found to reverse the phenomenon of increased porosity.

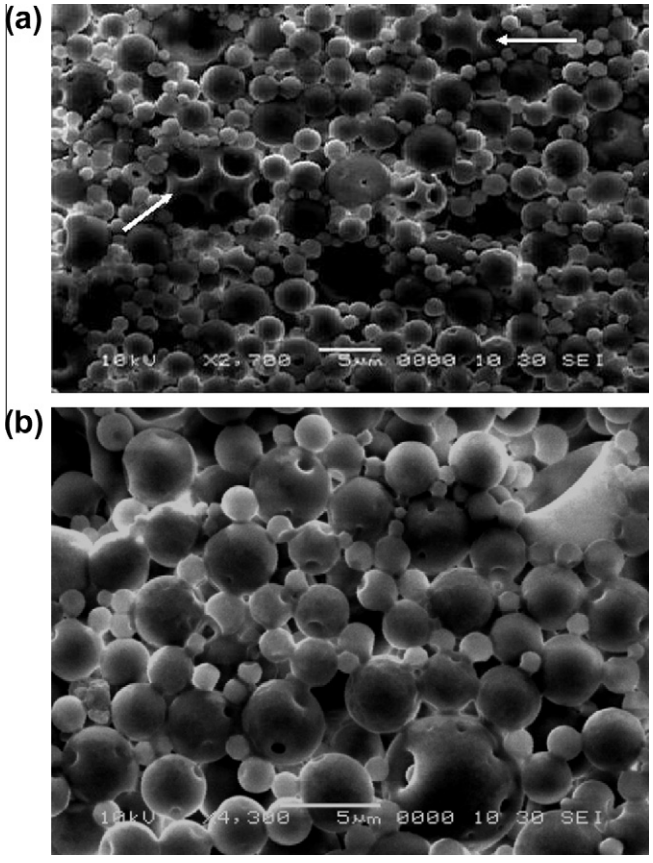

Fig. 2. (a) and (b): SEM micrographs of formula F4 at 2700× and 4300× magnifications, respectively. (For interpretation of the references to colour in this figure legend, the reader is referred to the web version of this article.)

In the SEM micrographs, the absence of drug crystals suggested the presence of the drug in an amorphous form.

3.4. Particle size analysis

Ideally, the geometric particle size of the microspheres should exceed 3 μm in order to escape phagocytosis by alveolar macrophages [1,33,34]. As obvious from the results in Table 2, the distribution modal size of the produced microspheres ranged from 3.68 to 10.48 μm. The increased NaCl concentration in the internal aqueous phase resulted in a significant increase in the particle size of the porous microspheres ($P < 0.05$). This could be attributed to the influx of water from the external to the internal aqueous phase in accordance with the osmotic gradient, leading to the enlargement and swelling of the internal aqueous droplets and resulting in an accompanying increase in the particle size of the produced microspheres [4]. On the other hand, the increased NaCl concentration in the external aqueous phase relative to the internal aqueous phase reverses the movement of water toward the external medium causing shrinkage of the internal aqueous droplets and an accompanying decrease in the particle size of the produced microspheres [4]. This came in accordance with Florence and Whitehill [3] who reported that the organic phase of a w/o/w emulsion acts as semipermeable membrane allowing the passage of water across the organic phase. This leads to either swelling or shrinkage of the internal droplets, depending on the direction of the osmotic gradient.

As also obvious from Table 2, some formulae exhibited bimodal size distribution. The least polydispersity as well as monomodal size was obtained with group III microspheres.

3.5. Particle flow and aerodynamic properties

The prepared microsphere groups showed a density range from 0.308 to 0.403 g/ml, suggesting their potential successful use for pulmonary delivery. In general, the highest density values were obtained by microsphere groups II and III followed by group I as shown in Fig. 5. These results were in agreement with the porosity and/or surface modifications of the particles as shown by SEM, in which microsphere groups II and III showed a rather nonporous surface while group I microspheres showed a porous surface. The osmotic pressure difference rather than the amount of NaCl in either the internal or external phase affected the density values. The higher the osmotic pressure difference between the internal and external aqueous phases, the lower the density, regardless of the direction of movement of water. However, the decrease in density values was found to be statistically insignificant ($P > 0.05$).

More importantly, the $MMAD_{th}$ of the formulations ranged from 2.24 to 5.86 μm, which was below the maximum value (6 μm) required for aerosolized particles to achieve efficient deposition in the lungs as proposed by Edwards et al. [33]. However, to achieve alveolar targeting of the microspheres for systemic absorption of

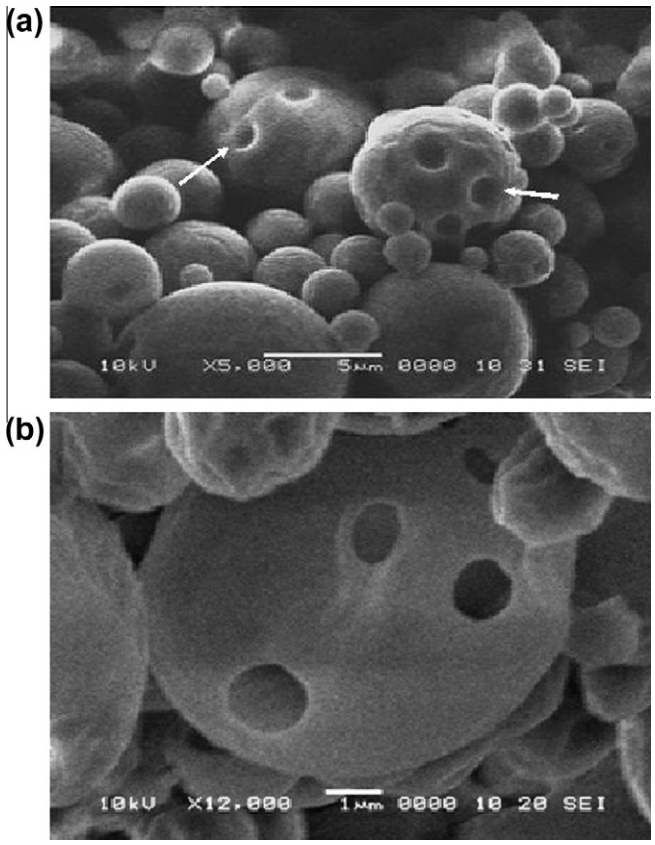

Fig. 3. (a) and (b): SEM micrographs of formula E1 at 5000× and 12,000× magnifications, respectively. (For interpretation of the references to colour in this figure legend, the reader is referred to the web version of this article.)

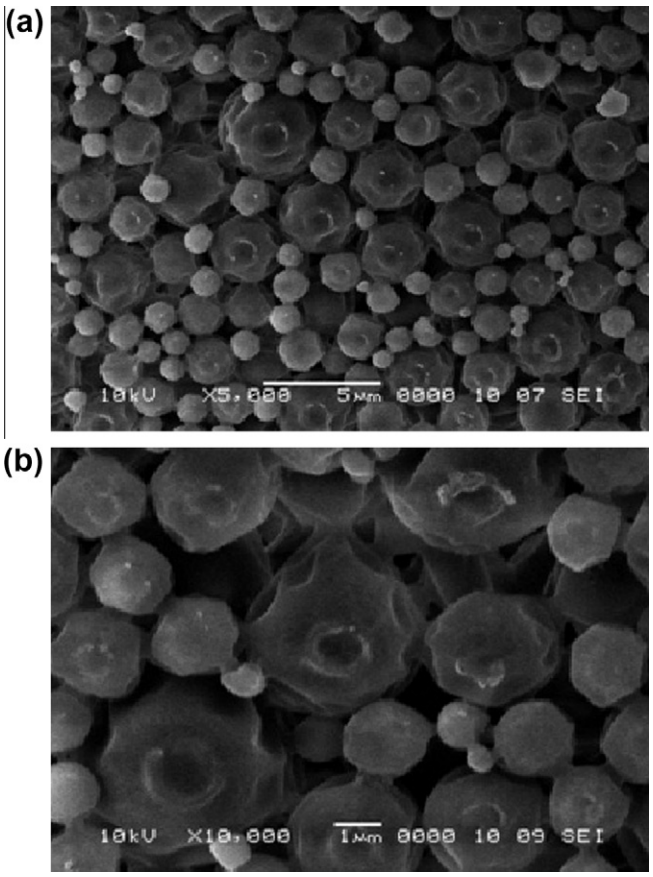

Fig. 4. (a) and (b): SEM micrographs of formula S5 at 5000× and 10,000× magnifications. (For interpretation of the references to colour in this figure legend, the reader is referred to the web version of this article.)

RS, the desirable aerodynamic diameter range was reported to be from 1 to 3 μm [21]. An aerodynamic diameter lying within this range was achieved by microspheres of group III.

Group I microspheres showed poor to very poor flow properties, and group II showed very poor to extremely poor flow properties. Both were typical micronized particle behavior in being very cohesive and of poor flow properties, since they exhibited somehow smooth surface [35]. Surprisingly, group III showed good to fair flow properties owing to the notched surface and nonsmooth structure. The modified surface morphology was reported by Chan and Chew [36] to improve the dispersibility of the microparticles owing to the reduced cohesion and the less close contact between the particles. This surface dimpling was considered advantageous to improve particle dispersion and aerosolization via reduction in particle–particle contact energies [37]. This came in accordance with Healy et al. [14] who reported that particle engineering techniques may be utilized to optimize the micromeritic properties of the particles to counteract cohesiveness and poor flowability/dispersion associated with microparticles.

3.6. In vitro drug release from microspheres

Owing to the complex nature of the release from PLA/PLGA systems, a range of models, involving contributions from either diffusion or polymer degradation, have been proposed in an attempt to quantify and predict drug release from biodegradable microparticles [38–40]. The number of phases exhibited in the drug release profile from PLA/PLGA systems depends on the porosity or the hydrophilicity of the microsphere system as well as the degree of interaction of the drug with the polymer. The free RS used as a control was completely released within the first 4 h. As evident from

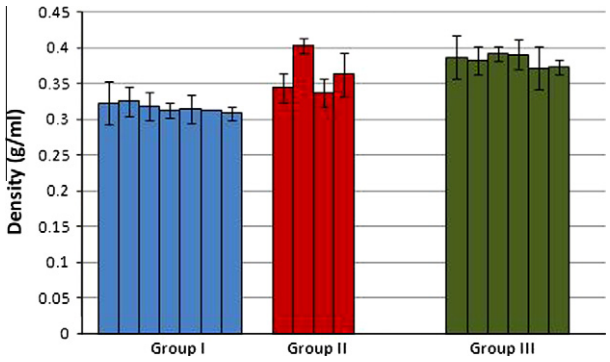

Fig. 5. Effect of the osmotic pressure difference created by NaCl concentration on the density of RS microspheres. (For interpretation of the references to colour in this figure legend, the reader is referred to the web version of this article.)

Table 2, microspheres prepared using PLGA 50:50 lead to a general significant increase in the released amount of RS than those prepared using PLGA 75:25 ($P < 0.05$). This concurred with the EE% results, owing to the higher content of glycolic acid in PLGA 50:50, which accelerated the degradation rate and presumably the uptake of water more than PLGA 75:25 [41]. The cumulative amount released after 15 days as shown in Fig. 6a–c could be arranged in the following decreasing order: group III microspheres > group I microspheres > group II microspheres. This could be interpreted based on the SEM micrographs, which showed that group III showed deep surface dimpling that could be responsible for this increased amount release of RS [42]. Similarly, the spongy and

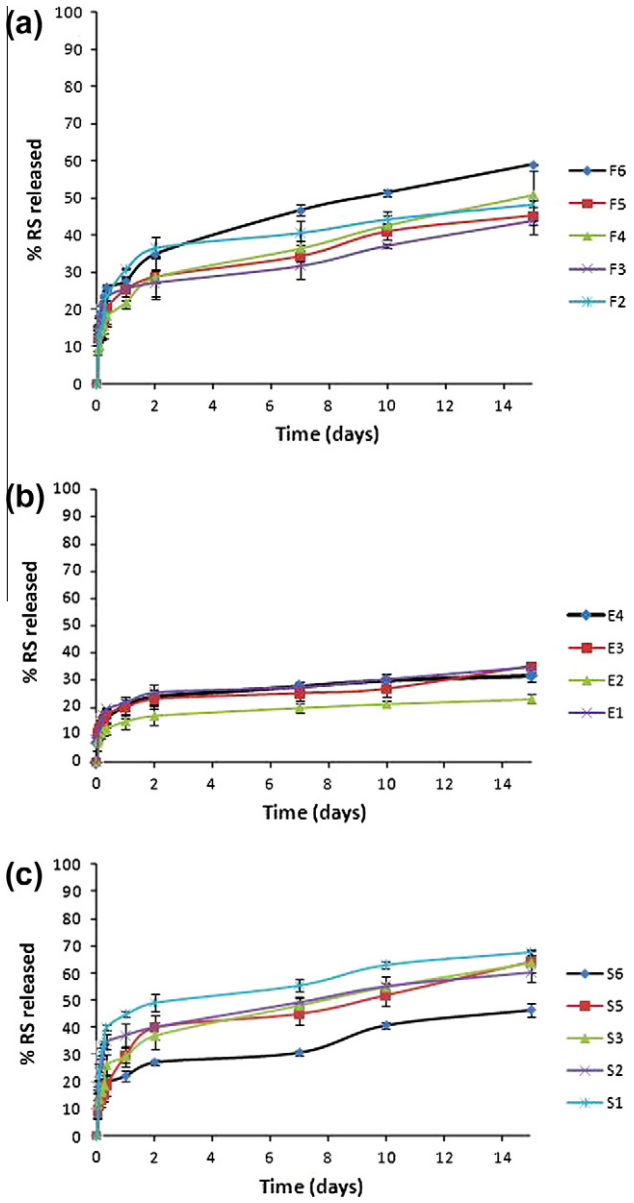

Fig. 6. (a–c): Release profiles of different microspheres formulae of groups I–III, respectively. (For interpretation of the references to colour in this figure legend, the reader is referred to the web version of this article.)

porous nature of group I microspheres lead to the relatively higher amount of RS released compared to group II microspheres, which showed only shallow surface dimpling and thus, exhibited a similar release behavior to nonmodified microspheres. The release of RS from microspheres exhibited a biphasic nature, which was a common finding with researchers studying the release from PLGA microparticulate systems [16,17]. Upon kinetic treatment of the release data, microspheres were shown to follow Fickian diffusion controlled release. It is worth noting that the controlled particle porosity preparation exerted through NaCl addition in the external aqueous phase resulted in burst suppression and an effective modulation of the overall release.

3.7. Microspheres true density and SSA

Formulae F4, E1, and S5 were chosen as representatives of groups I–III, respectively. Results of this experiment are illustrated in Table 3. The SSA of formulae F4 and S5 was higher than that of E1, concurring with the results of particle flow and *in vitro* release experiments. Formula E1 that is neither surface engineered nor possessing porous nature had the lowest SSA value, while formulae F1 and S5 had higher SSA owing to the porous and dimpled surface, respectively, confirming SEM observations.

Table 3
The true density and specific surface area (SSA) of selected RS loaded microspheres.

Formula	True density* (gm/cm^3)	SSA (m^2/g)
F4	1.395 ± 0.04	2.795 ± 0.09
E1	1.342 ± 0.04	1.841 ± 0.06
S5	1.358 ± 0.06	2.667 ± 0.12

* measured by helium pycnometry.

3.8. Differential scanning calorimetry (DSC)

The DSC thermogram of the selected RS loaded formulae F4, E1, and S5 suggests that RS is most probably in an amorphous form, manifested by the disappearance of its endothermic peaks in the encapsulated form (Supplementary Material). A shift in the polymer's T_g from 45.94 °C to higher values in the prepared microspheres suggests the arrangement of polymer molecules around the drug molecules forming a rigid structure (Supplementary Material). This finding also suggests the creation of a diffusion barrier to the drug by the hydrophobic long alkyl chains of the polymers, hence assuring prolonged drug release.

3.9. MTT assay

Concerns regarding the safety and clearance of the polymers and excipients from the lungs constitute one of the major reasons for the delay of commercialization of controlled pulmonary drug delivery systems. A large group of polymers and excipients have received the G.R.A.S (Generally Regarded As Safe) status from the US FDA. However, not all of them can be considered absolutely safe to the lung as the toxicity of a substance varies greatly with the route of administration (i.e., excipients considered to be safe for ingestion could not be safe for inhalation), and in addition, the drug delivery system may also present some toxicological concerns. Cell viability tests provide a reliable gross estimate of the cell response to an insult and therefore are used as a biocompatibility assessment criterion [43].

Results of the MTT assay, performed on the selected formula S5 in drug loaded and blank forms, are presented in Fig. 7. SLS, serving as the positive control, resulted in a significant decrease in cell viability at all concentrations with IC_{50} of 440.9 μg/ml. RS was found

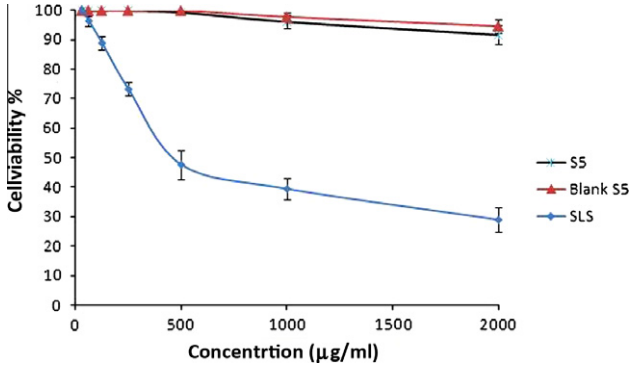

Fig. 7. Cell viability% of Calu-3 cells for formulae S5 in drug loaded and blank forms as compared to SLS. (For interpretation of the references to colour in this figure legend, the reader is referred to the web version of this article.)

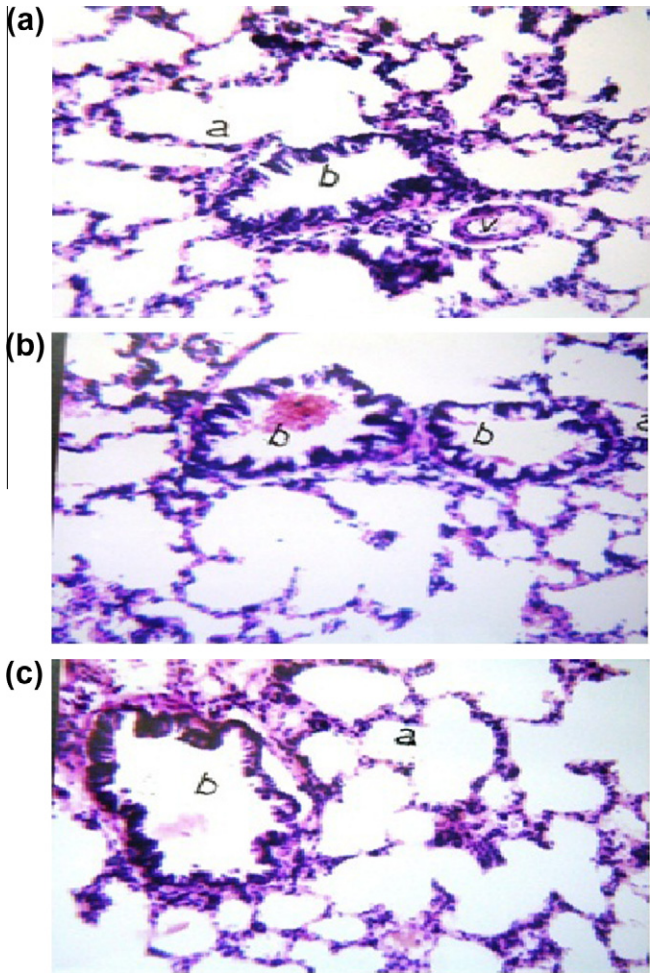

Fig. 8. (a–c): The histology of rat lung tissue after intra-tracheal administration of: (a) PBS as a negative control, (b) 1 mg RS in solution form, and (c) formula S5 in an amount equivalent to 1 mg RS, respectively. (For interpretation of the references to colour in this figure legend, the reader is referred to the web version of this article.)

to be safe on Calu-3 cells up to a concentration of 500 μg/ml, followed by a decrease in cell viability to 95.1% and 87.2% at a concentration of 1000 and 2000 μg/ml, respectively. Formula S5 exhibited a similar behavior and was completely safe up to a concentration of 500 μg/ml followed also by a respective decrease in cell viability to 96.2% and 91.6% at 1000 and 2000 μg/ml concentrations, respectively.

3.10. Histopathological examination of rat lung tissue

Pathological lung alteration would result in the appearance of inflammatory cell infiltration, necrosis and damage to the cells, perivascular edema, and the possibility of localized intra-alveolar bleeding [44], As evident from Fig. 8a–c representing groups I, II and III, respectively, no histopathological alteration of lung tissue occurred after 24 h of administration of RS either in solution form or in the encapsulated form (formula S5). This finding suggests the safety of the drug and the formula on the lung tissue.

3.11. In vitro aerosolization study

The deposition percentage of RS onto different stages of the NGI, the capsule, and the adapter using the Aerolizer® device is illustrated in Fig. 9. The EF% of formula S5 was found to be 90.5% ± 3.20, while the FPF% was found to be 62.94% ± 2.65. The calculated MMAD was 2.31 ± 0.03 μm, which was close to the one obtained by theoretical calculation (2.24 μm).

The data obtained from the aerosolization study confirmed appropriate powder flow manifested by the high EF%. Moreover, deep lung deposition potential previously suggested by the theoretically calculated aerodynamic diameter was further confirmed by the high value of FPF%.

3.12. In vivo determination of the amount of bone deposited ^{125}I-RS

The reaction conditions utilized for radiolabeling of RS allowed a high reaction yield (over 90%) to be obtained. Upon performing TLC, the free iodide remained near the origin with R_f = 0–0.3, while the labeled RS migrated with the solvent front with R_f = 0.6.

Results of the *in vivo* study presented in Table 4 revealed the presence of RS in the blood after 24 h after both IV and orotracheal instillation, which may be attributed to its binding to the plasma proteins owing to its complete ionization at physiologic pH 7.4 [45]. Following IV administration, about 43% of RS was deposited in the bones, owing to the selective binding of RS to the hydroxyapatite crystals. The statistically nonsignificant difference between the amount deposited in the bones after 24 h and 7 days was

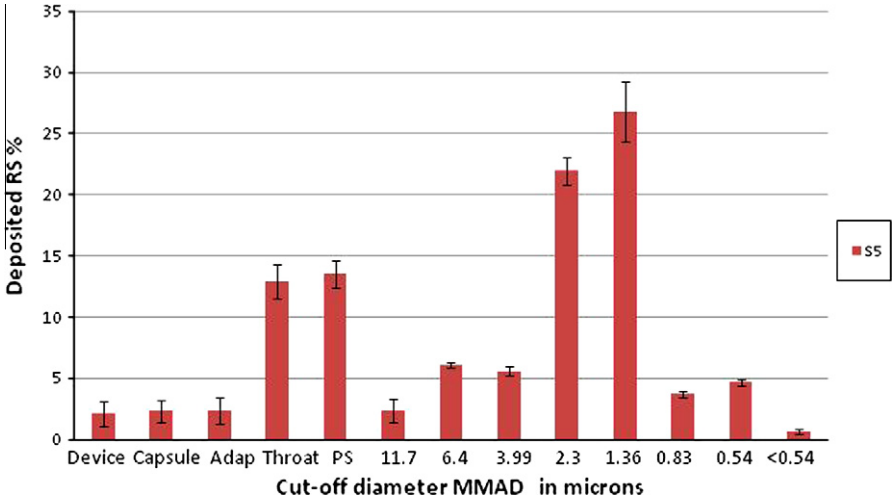

Fig. 9. *In vitro* deposition pattern of formula S5 using NGI at a flow rate 30 l/min and Aerolizer® as inhaler device. (For interpretation of the references to colour in this figure legend, the reader is referred to the web version of this article.)

Table 4
The percentage of injected/inhaled dose of RS in blood, bone, and thyroid gland following IV and pulmonary administration.

	% I.D. (Mean ± S.E.)			
	Values after 24 h		Values after 7 days	
	Group I*	Group III**	Group II*	Group IV**
Blood	5.22 ± 0.67	4.39 ± 1.10	0 ± 0.00	0 ± 0.00
Bone	14.88 ± 0.05	43.20 ± 2.05	33.96 ± 3.19	43.83 ± 3.20
Thyroid gland	0.30 ± 0.02	0.17 ± 0.02	0.001 ± 0.00	0.02 ± 0.002

* Intra-tracheal administration.
** IV administration.

attributed to the fact that upon IV administration, BPs are rapidly uptaken by the bones and the rest of the dose (about 30–80%) is excreted in the urine within 24 h [10]. In contrast, after intra-tracheal instillation, about 15% of RS was deposited in the bones after 24 h followed by an increase to about 34% after 7 days. This finding confirmed the sustained release nature of the produced microspheres. The high value deposited in the bones after pulmonary administration of RS as compared to IV administration suggests that the pulmonary route is a suitable alternative to oral route. The low radioactivity values in the thyroid gland prove the *in vivo* stability of radiolabeled RS [46].

4. Conclusions

The utilization of NaCl as an osmogen in the w/o/w double emulsion technique leads to morphologically diverse microspheres. The increased concentration of NaCl in the external phase was proven to be advantageous in producing dimpled microspheres of high EE%, suitable particle size both geometrically and aerodynamically, good flow properties, and a sustained release profile. While more work is needed to extrapolate these findings to better anti-osteoporotic efficacy by pulmonary route, regarding the therapeutic dosing and safety, the presented study is encouraging and clearly offers an alternative to oral administration of RS with regard to sustainability and enhanced BPs bone deposition.

Acknowledgment

The authors would like to thank SPIC Pharma Co., India, and PURAC company, the Netherlands, for their kind supply of risedronate and PLGA polymers, respectively.

Appendix A. Supplementary material

Supplementary data associated with this article can be found, in the online version, at doi:10.1016/j.ejpb.2011.07.010.

References

[1] J. Lee, Y.J. Oh, S.K. Lee, K.Y. Lee, Facile control of porous structures of polymer microspheres using an osmotic agent for pulmonary delivery, J. Control. Rel. 146 (2010) 61–67.
[2] S. Samdancioglu, S. Calis, M. Sumnu, A. Atilla Hincal, Formulation and *in vitro* evaluation of bisphosphonate loaded microspheres for implantation in osteolysis, Drug Dev. Ind. Pharm. 32 (2006) 473–481.
[3] A.T. Florence, D. Whitehill, The formulation and stability of multiple emulsions, Int. J. Pharm. 11 (1982) 277–308.
[4] K.-F. Pistel, T. Kissel, Effects of salt addition on the microencapsulation of proteins using w/o/w double emulsion technique, J. Microencapsul. 17 (2000) 467–483.
[5] M.R. Allen, Skeletal accumulation of bisphosphonates: implications for osteoporosis treatment, Expert Opin. Drug Metab. Toxicol. 4 (2008) 1371–1378.
[6] S. Adami, N. Zamberlan, Adverse effects of bisphosphonates. A comparative review, Drug Saf. 14 (1996) 158–170.
[7] C.P. Peter, L.K. Handt, S.M. Smith, Esophageal irritation due to alendronate sodium tablets: possible mechanisms, Dig. Dis. Sci. 43 (1998) 1998–2002.
[8] M.A. Blank, B.L. Ems, G.W. Gibson, W.R. Myers, S.K. Berman, R.J. Phipps, P.N. Smith, Non clinical model for assessing gastric effects of bisphosphonates, Dig. Dis. Sci. 42 (1997) 281–288.
[9] W.A. Blumentals, S.T. Harris, R.E. Cole, L. Haung, S.L. Silverman, Risk of severe gastrointestinal events in women treated with monthly ibandronate or weekly alendronate and risedronate, Ann. Pharmacother. 43 (2009) 577–585.
[10] A. Ezra, G. Golomb, Administration routes and delivery systems of bisphosphonates for the treatment of bone resorption, Adv. Drug Deliv. Rev. 42 (2000) 175–195.
[11] M.A. Blank, G.W. Gibson, W.R. Myers, T.A. Dierckman, R.J. Phipps, P.N. Smith, Gastric damage in the rat with nitrogen-containing bisphosphonates depends on pH, Aliment. Pharmacol. Ther. 14 (2000) 1215–1223.
[12] M. Nasr, G.A.S. Awad, S. Mansour, A. Al Shamy, N.D. Mortada, A reliable predictive factorial model for entrapment optimization of a sodium bisphosphonate into biodegradable microspheres, J. Pharm. Sci. 100 (2011) 612–621.
[13] B. Bittner, M. Morlock, H. Koll, G. Winter, T. Kissel, Recombinant human erythropoietin (rhEPO) loaded poly(lactide-co-glycolide) microspheres: influence of the encapsulation technique and polymer purity on microsphere characteristics, Eur. J. Pharm. Biopharm. 45 (1998) 295–305.
[14] A.M. Healy, B.F. McDonald, L. Tajber, O.I. Corrigan, Characterisation of excipient-free nanoporous microparticles (NPMPs) of bendroflumethiazide, Eur. J. Pharm. Biopharm. 69 (2008) 1182–1186.
[15] L.M. Nolan, L. Tajber, B.F. McDonald, A.S. Barham, O.I. Corrigan, A.M. Healy, Excipient-free nanoporous microparticles of budesonide for pulmonary delivery, Eur. J. Pharm. Sci. 37 (2009) 593–602.
[16] F. Ungaro, R. d'Emmanuele di Villa Bianca, C. Giovino, A. Miro, R. Sorrentino, F. Quaglia, M.I. La Rotonda, Insulin-loaded PLGA/cyclodextrin large porous particles with improved aerosolization properties: *in vivo* deposition and hypoglycaemic activity after delivery to rat lungs, J. Control. Rel. 135 (2009) 25–34.
[17] F. Ungaro, G. De Rosa, A. Miro, F. Quaglia, M.I. La Rotonda, Cyclodextrins in the production of large porous particles: development of dry powders for the sustained release of insulin to the lungs, Eur. J. Pharm. Sci. 28 (2006) 423–432.
[18] A. Rawat, Q.H. Majumder, F. Ahsan, Inhalable large porous microspheres of low molecular weight heparin: *in vitro* and *in vivo* evaluation, J. Control. Rel. 128 (2008) 224–232.
[19] F. Ungaro, C. Giovino, C. Coletta, R. Sorrentino, A. Miro, F. Quaglia, Engineering gas-foamed large porous particles for efficient local delivery of macromolecules to the lung, Eur. J. Pharm. Sci. 41 (2010) 60–70.
[20] R.O. Cook, R.K. Pannu, I.W. Kellaway, Novel sustained release microspheres for pulmonary drug delivery, J. Control. Rel. 104 (2005) 79–90.
[21] N. Sivadas, D. O'Rourke, A. Tobin, V. Buckley, Z. Ramtoola, J.G. Kelly, A.J. Hickey, S.-A. Cryan, A comparative study of a range of polymeric microspheres as potential carriers for the inhalation of proteins, Int. J. Pharm. 358 (2008) 159–167.
[22] N.A. Peppas, Analysis of Fickian and non-Fickian drug release from polymers, Pharm. Acta Helv. 60 (1985) 110–111.
[23] K. Vay, S. Scheler, W. Friess, New insights into the pore structure of poly(D,L-lactide-co-glycolide) microspheres, Int. J. Pharm. 402 (2010) 20–26.
[24] Y. Bahl, H. Sah, Dynamic changes in size distribution of emulsion droplets during ethyl acetate-based microencapsulation process, AAPS Pharm. Sci. Technol. 1 (2000) E5.
[25] F. Tewes, J. Brillault, W. Couet, J.-C. Olivier, Formulation of rifampicin-cyclodextrin complexes for lung nebulization, J. Control. Rel. 129 (2008) 93–99.
[26] M. Taki, C. Marriott, X.-M. Zeng, G.P. Martin, Aerodynamic deposition of combination dry powder inhaler formulations *in vitro*: a comparison of three impactors, Int. J. Pharm. 388 (2010) 40–51.
[27] I.M. El-Sherbiny, H.D. Smyth, Biodegradable nano-micro carrier systems for sustained pulmonary drug delivery: (I) self-assembled nanoparticles encapsulated in respirable/swellable semi-IPN microspheres, Int. J. Pharm. 395 (2010) 132–141.
[28] A.M. Amin, S.E. Soliman, H.A. El-Aziz, Preparation and biodistribution of [^{125}I] Melphalan: a potential radioligand for diagnostic and therapeutic applications, J. Label. Compd. Radiopharm. 53 (2010) 1–5.
[29] D.J. Maddalena, TISCON, A Basic Computer Program for the Calculation of the Biodistribution of Radionuclide-Labelled Drugs in Rats and Mice, Australian Atomic Energy Commission, Lucas Heights, Australia, 1983.
[30] P. Perugini, I. Genta, B. Conti, T. Modena, F. Pavanetto, Long-term release of clodronate from biodegradable microspheres, AAPS Pharm. Sci. Technol. 2 (2001) E10.
[31] T. Uchida, K. Yoshida, S. Goto, Preparation and characterization of polylactic acid microspheres containing water-soluble dyes using a novel w/o/w emulsion solvent evaporation method, J. Microencapsul. 13 (1996) 219–228.
[32] U. Weidenauer, D. Bodmer, T. Kissel, Microencapsulation of hydrophilic drug substances using biodegradable polyesters. Part II: Implants allowing controlled drug release – a feasibility study using bisphosphonates, J. Microencapsul. 21 (2004) 137–149.
[33] D.A. Edwards, J. Hanes, G. Caponetti, J. Hrkach, A. Ben-Jebria, M.L. Eskew, J. Mintzes, D. Deaver, N. Lotan, R. Langer, Large porous particles for pulmonary drug delivery, Science 276 (1997) 1868–1872.

[34] D.A. Edwards, A. Ben-Jebria, R. Langer, Recent advances in pulmonary drug delivery using large porous inhaled particles, J. Appl. Physiol. 85 (1998) 379–385.
[35] T. Sebti, K. Amighi, Preparation and *in vitro* evaluation of lipidic carriers and fillers for inhalation, Eur. J. Pharm. Biopharm. 63 (2006) 51–58.
[36] H.K. Chan, N.Y. Chew, Novel alternative methods for the delivery of drugs for the treatment of asthma, Adv. Drug Deliv. Rev. 55 (2003) 793–805.
[37] F. Mohamed, C.F. van der Walle, PLGA microcapsules with novel dimpled surfaces for pulmonary delivery of DNA, Int. J. Pharm. 311 (2006) 97–107.
[38] J. Siepmann, A. Göpferich, Mathematical modeling of bioerodible, polymeric drug delivery systems, Adv. Drug Deliv. Rev. 48 (2001) 229–247.
[39] N. Faisant, J. Siepmann, J.P. Benoit, PLGA-based microparticles: elucidation of mechanisms and a new, simple mathematical model quantifying drug release, Eur. J. Pharm. Sci. 15 (2002) 355–366.
[40] D.Y. Arifin, L.Y. Lee, C.H. Wang, Mathematical modeling and simulation of drug release from microspheres: Implications to drug delivery systems, Adv. Drug Deliv. Rev. 58 (2006) 1274–1325.
[41] F. Cui, D. Cun, A. Tao, M. Yang, K. Shi, M. Zhao, Y. Guan, Preparation and characterization of melittin-loaded poly (DL-lactic acid) or poly (DL-lactic-co-glycolic acid) microspheres made by the double emulsion method, J. Control. Rel. 107 (2005) 310–319.
[42] H. Yoshizawa, S. Nishino, K. Shiomori, S. Natsugoe, T. Aiko, Y. Kitamura, Surface morphology control of polylactide microspheres enclosing irinotecan hydrochloride, Int. J. Pharm. 296 (2005) 112–116.
[43] C.F. Jones, D.W. Grainger, *In vitro* assessments of nanomaterial toxicity, Adv. Drug Deliv. Rev. 61 (2009) 438–456.
[44] H. Katsumi, M. Nakatani, J. Sano, M. Abe, K. Kusamori, M. Kurihara, R. Shiota, M. Takashima, T. Fujita, T. Sakane, T. Hibi, A. Yamamoto, Absorption and safety of alendronate, a nitrogen-containing bisphosphonate, after intrapulmonary administration in rats, Int. J. Pharm. 400 (2010) 124–130.
[45] R.J. Milner, J. Farese, C.J. Henry, K. Selting, T.M. Fan, L.P. de Lorimier, Bisphosphonates and cancer, J. Vet. Intern. Med. 18 (2004) 597–604.
[46] E.A. EL-Ghany, A.M. Amine, A.S. EL-Sayed, M.T. EL-Kolaly, F. Abdel-Gelil, Radiochemical and biological characteristics of radioactive iodine labeled indomethacin for imaging of inflammation, J. Radioanal. Nucl. Chem. 266 (2005) 117–124.